Supporting Information for:
Structural evolution and stability of Sc2(WO4)3 after discharge in a sodium-based electrochemical cell

Henrik L. Andersen,[a,b] Othman K. Al Bahri,[b] Sergey Tsarev,[c] Bernt Johannessen,[d] Bernd Schulz,[b] Junnan Liu,[b] Helen Brand,[d] Mogens Christensen[a] and Neeraj Sharma[b]*

[a] Center for Materials Crystallography, Dept. of Chemistry and iNANO, Aarhus University, DK-8000 Aarhus C, Denmark
[b] School of Chemistry, UNSW Australia, Sydney NSW 2052, Australia
[c] School of Civil and Environmental Engineering, UNSW Australia, Sydney, NSW 2052, Australia
[d] Australian Synchrotron, Clayton, Victoria 3168, Australia

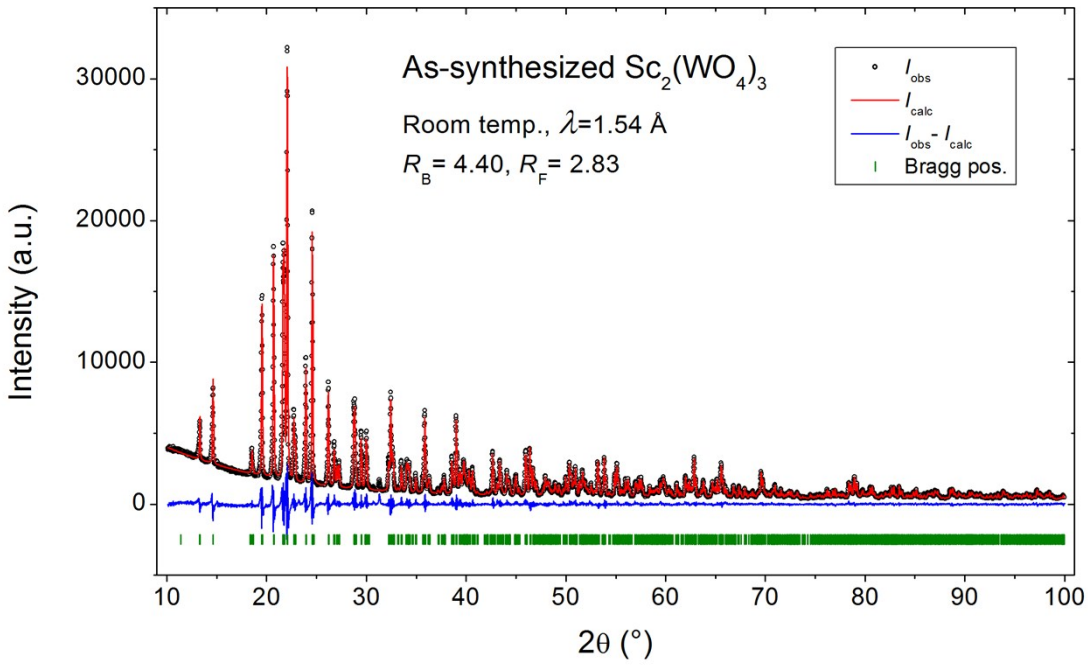

Figure S1. Room temperature PXRD patterns of the as-synthesized $Sc_2(WO_4)_3$ modeled by the Rietveld method.

	***a* (Å)**	***b* (Å)**	***c* (Å)**	**Vol (Å³)**
$Sc_2(WO_4)_3$	9.66904(5)	13.31786(8)	9.57720(5)	1233.27(2)

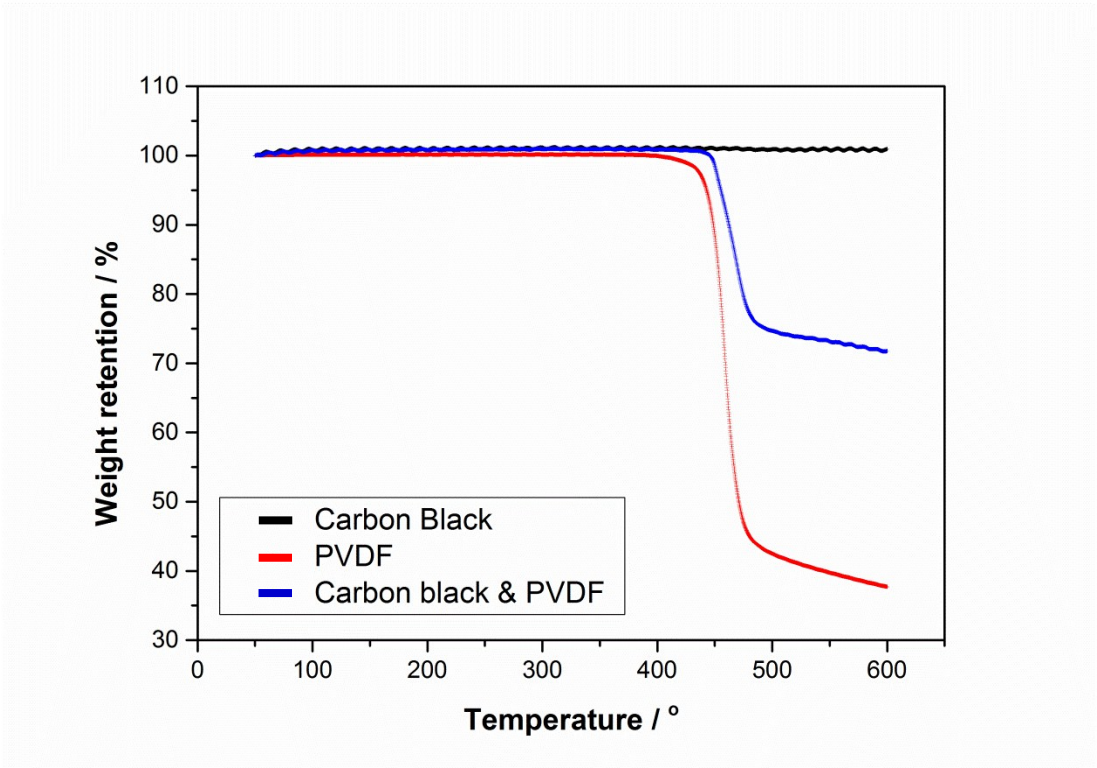

Figure S2. Thermogravimetric data of carbon black, PVDF and the carbon black/PVDF mixture.

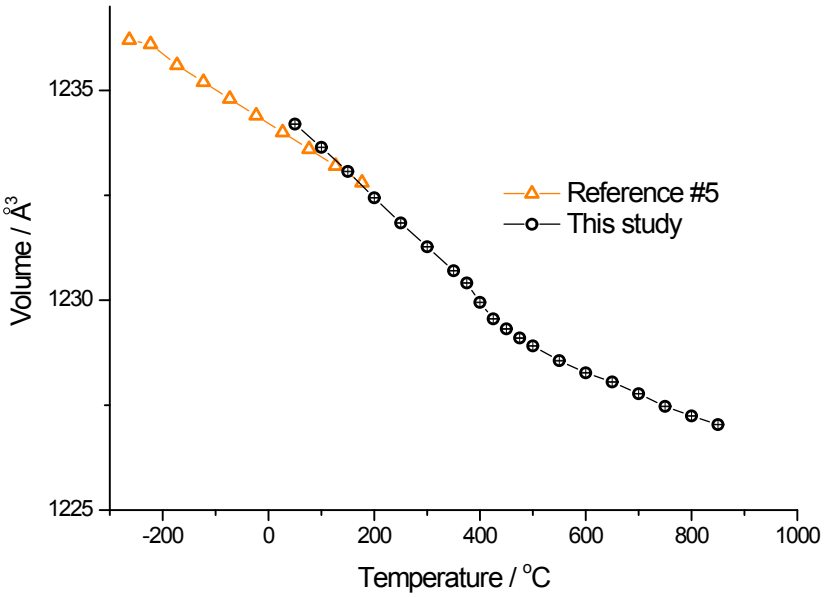

Figure S3. Comparison of the refined volume of $Sc_2(WO_4)_3$ from [5] and from our work. In our case the thermal evolution corresponds to the electrode, $Sc_2(WO_4)_3$/PVDF/carbon black.

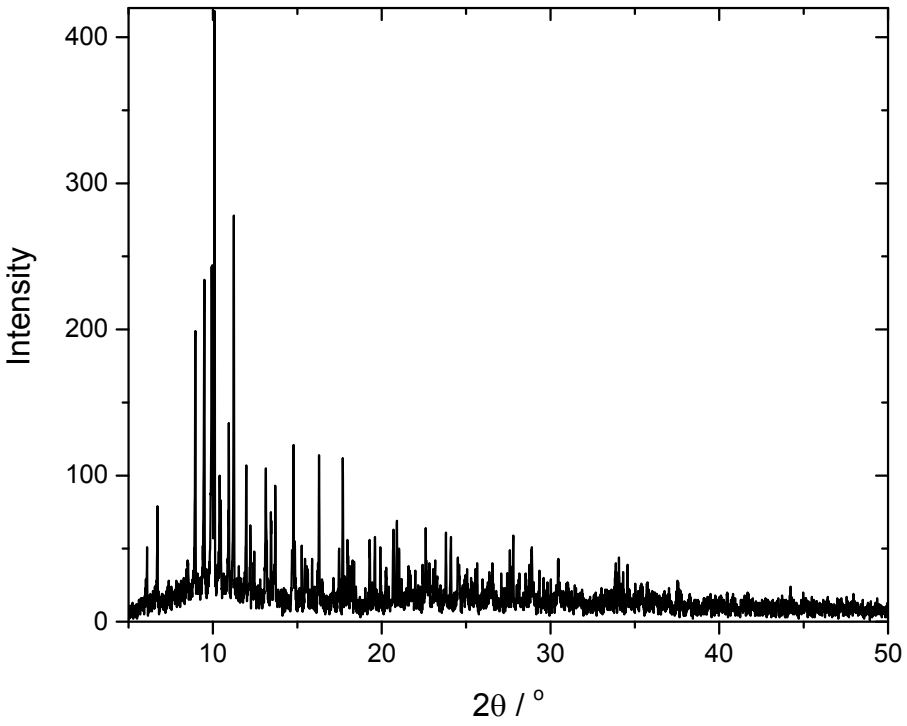

Figure S4. Representative XRD pattern of data collected during the low temperature experiments.

Indexing of unknown phases

Preliminary Indexing and assignment of unknown reflections in the variable temperature data of SWO 50% discharge and SWO 75% discharge to potential phases were carried out manually based on the thermal evolution (appearance/disappearance of the same series of peaks) and the peak profiles (see Figure S5 and Figure S6). The patterns have been normalized by the maximum peak intensity to allow comparison between the crystalline starting powder and the highly amorphous high temperature data.

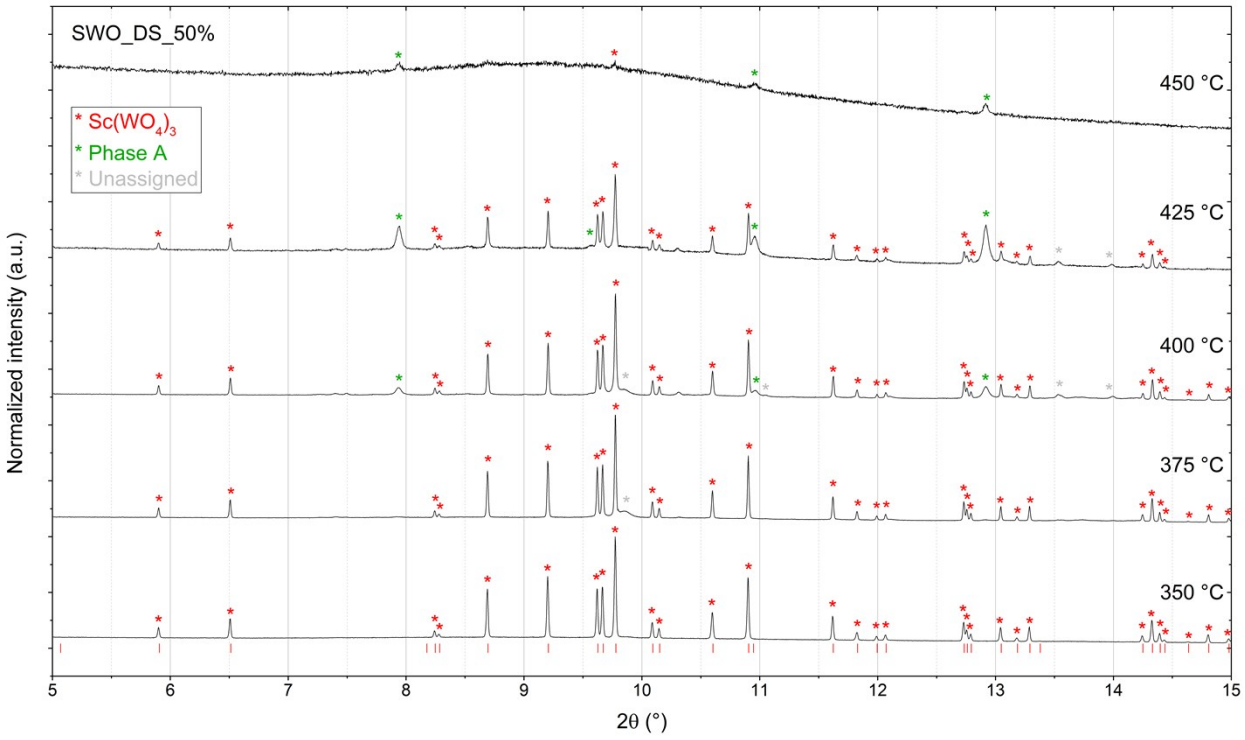

Figure S5. Indexed phases in the SWO 50% discharge with the variable temperature data. The red ticks at the bottom indicate the Bragg positions of the main $Sc_2(WO_4)_3$ phase.

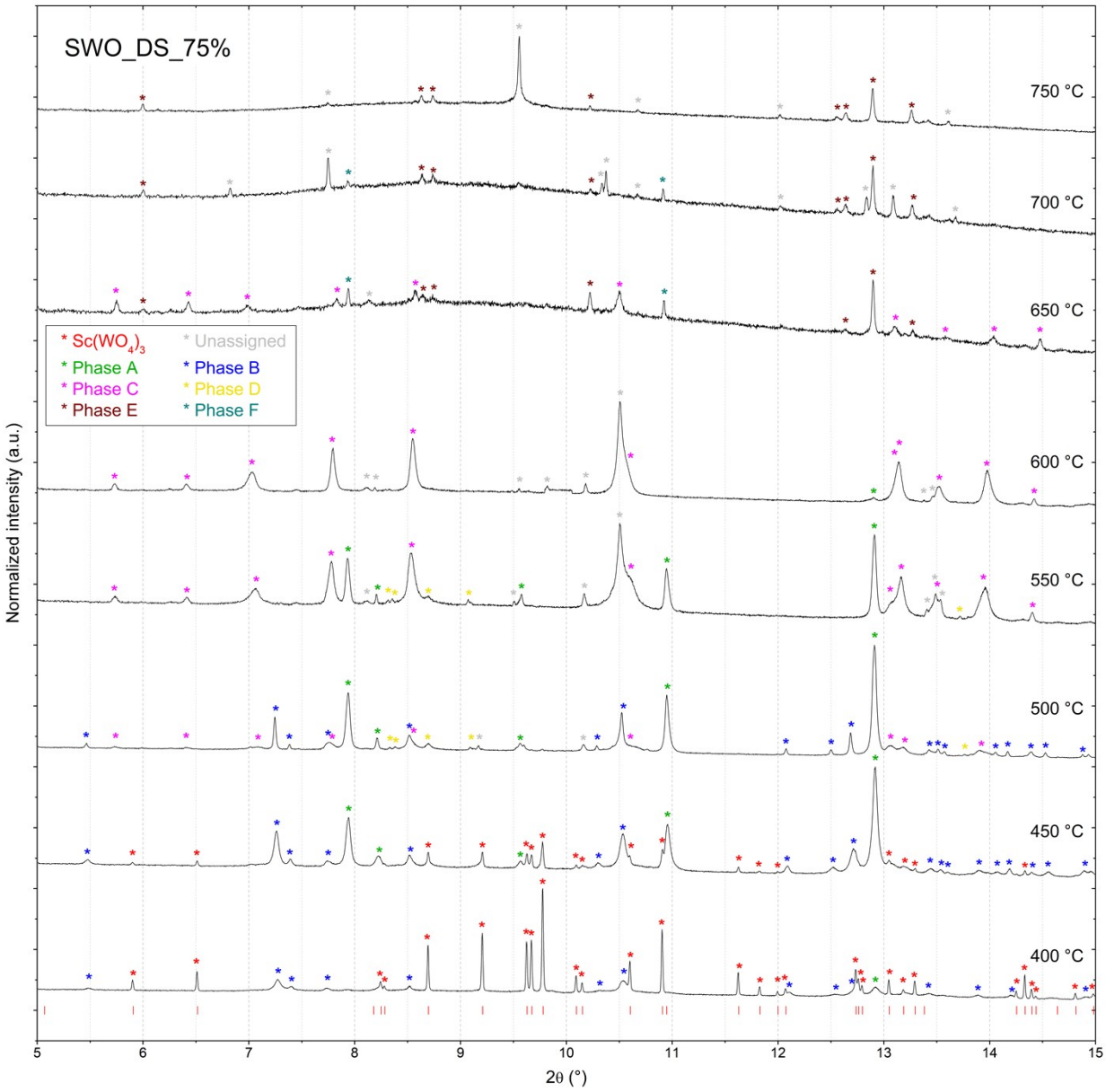

Figure S6. Indexed phases in the SWO 75% discharge variable temperature data. The red ticks at the bottom indicate the Bragg positions of the main $Sc_2(WO_4)_3$ phase.

For SWO 50% discharge sample substantial amorphization occurs when heating above 425 °C and only one phase, Phase A, could be assigned in addition to the main $Sc_2(WO_4)_3$ phase. For SWO 75% discharge a series of phase transitions can be seen in the data. A total of six different phases were indexed in the data between 400 and 750 °C. Notably, Phase A (green ticks) was found to be present in both SWO 50% and SWO 75% discharge.

Unit cell determination

The software Expo2014[1] and DICVOL06[2] were used in an attempt to determine the unit cell parameters of the three most pronounced unknown phases in the variable temperature PXRD data from the manually indexed unknown phases.

Phase A

The main peak of Phase A at ~12.9° appears as a broad peak at 400 °C in both SWO 50% and SWO 75% discharge data. In the SWO 50% discharge, Phase A peaks sharpen and in the highly amorphous data at 450 °C only the three main peaks of phase A and a hint of the most intense peak of $Sc_2(WO_4)_3$ can be seen. In the SWO 75% discharge, the peaks of Phase A sharpen at 450 °C, and are present at 500 and 550 °C, but disappears at 600 °C. The unit cell search was carried out using the peak positions indexed to Phase A in the SWO 75% discharge data at 500 °C. The unit cell search in DICVOL06 was performed using a peak position error of 0.010°, maximum unit cell volume of 4000 Å^3, and a refinable zero shift. Cubic, tetragonal, hexagonal, orthorhombic and monoclinic crystal systems were tested in the search. The top three results are given in the table below.

Nr.	Sym.	*a* (Å)	*b* (Å)	*c* (Å)	alpha (°)	beta (°)	gamma (°)	Vol. (Å^3)	M20	Shift (°)
1	Ortho	14.8391	4.7873	4.1087	90	90	90	291.88	456.20	0.023
2	Hexa	6.1273	6.1273	28.9117	90	90	120	940.04	99.50	-0.032
3	Tetra	5.7797	5.7797	28.7730	90	90	90	964.17	56.00	0.014

As indicated by the M20 figure-of-merit, the best estimate of the unit cell of Phase A is an orthorhombic cell with *a* = 14.8391, *b* = 4.7873 and *c* = 4.1087 Å. The Bragg positions corresponding to this unit cell are indicated by the ticks in the figure below.

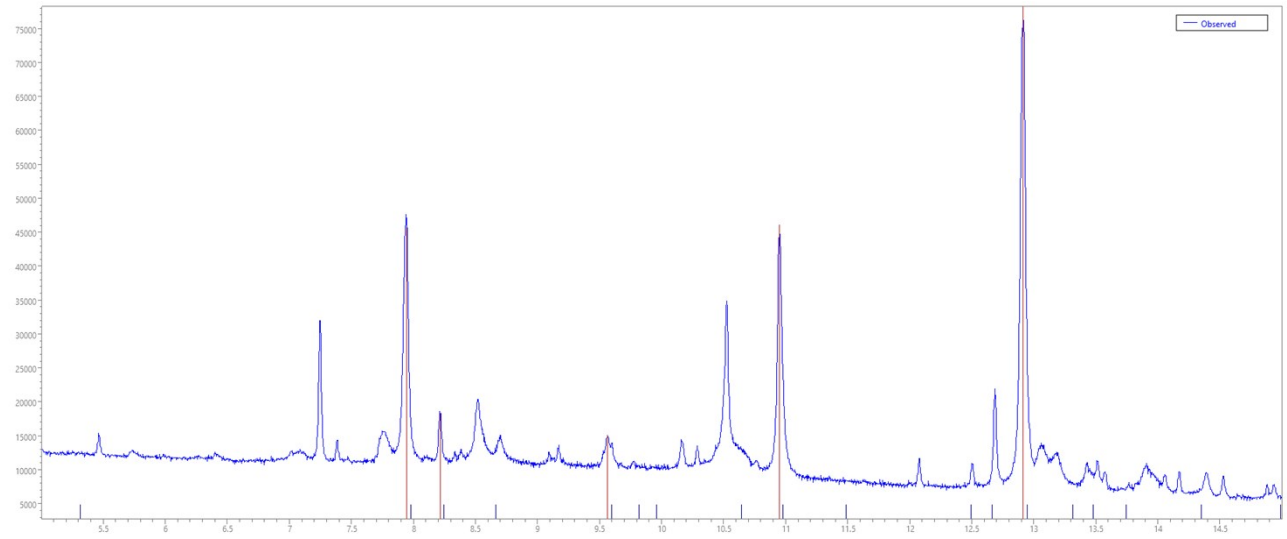

Figure S7. Selected region of the SWO 75% discharge at 500 °C diffraction pattern. The red lines indicate the indexed peak positions of phase A and the blue ticks in the bottom indicate the Bragg positions of the highest figure-of-merit orthorhombic unit cell.

Phase B

The peaks from Phase B appear at 400 °C in the SWO 75% discharge data initially as broad weak peaks. At 450 and 500 °C the peaks sharpen indicating grain growth, however at 550 °C the peaks from Phase B disappear. The unit cell search was carried out using the peak positions indexed to Phase B in SWO 75% discharge at 400 °C data. The unit cell search in DICVOL06 was performed using a peak position error of 0.010°, maximum unit cell volume of 4000 Å^3, and a refinable zero shift. Cubic, tetragonal, hexagonal, orthorhombic and monoclinic crystal systems were tested in the search. The top five results are given in the table below.

Nr.	Sym.	*a* (Å)	*b* (Å)	*c* (Å)	*alpha* (°)	*beta* (°)	*gamma* (°)	Vol. (Å^3)	M20	Shift (°)
1	Mono	14.9448	9.5998	7.1726	90	91.90	90	1028.46	20.60	-0.011
2	Mono	16.4927	3.8155	16.1306	90	122.77	90	853.54	18.50	0.002
3	Mono	16.4828	4.3360	15.6146	90	119.81	90	968.25	17.20	0.004
4	Mono	11.3233	10.9620	7.4874	90	106.91	90	889.19	16.80	0.007
5	Ortho	26.6527	15.7830	7.4656	90	90	90	3140.49	12.70	-0.008

The best estimate of the unit cell was achieved by a monoclinic cell with a = 14.9448, b = 9.5998, c = 7.1726 Å and β = 91.90°. However, no distinctly independent "best" result was achieved and no outstanding M20 figure-of-merits were attained for any of the tested unit cells.

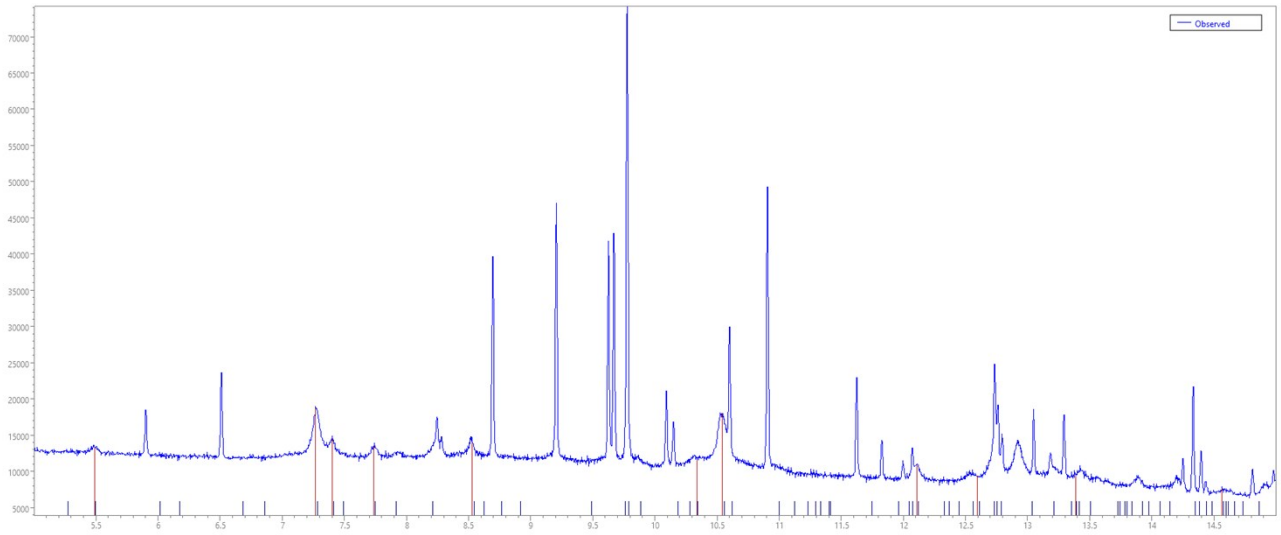

Figure S8. Selected region of the diffraction pattern of SWO 75% discharge at 400 °C. The red lines indicate the indexed peak positions of Phase B and the blue ticks in the bottom indicate the Bragg positions of the best figure-of-merit monoclinic unit cell in the search.

Phase C

The very broad peaks of Phase C (magenta ticks) are initially seen at 500 °C in the SWO 75% discharge data. The peaks sharpen and remain in the data at 550, 600 and 650 °C. The relative positions of the peaks seem to vary in a slightly anisotropic manner which could indicate an anistropic thermal expansion behavior. This can be seen, for example in the two initially distinct peaks at $2\theta \sim 13.2°$ at 500°C which merge into one peak at 600 °C. The unit cell search was carried out using the peak positions indexed to Phase C in the SWO 75% discharge at 600 °C data. The unit cell search in DICVOL06 was performed using a peak position error of 0.010°, maximum unit cell volume of 4000 Å^3, and a refinable zero shift. Cubic, tetragonal, hexagonal, orthorhombic and monoclinic crystal systems were tested in the search. The top four results are given in the table below.

Nr.	Sym.	*a* (Å)	*b* (Å)	*c* (Å)	alpha (°)	beta (°)	gamma (°)	Vol. (Å^3)	M20	Shift (°)
1	Mono	7.3755	13.8282	6.0073	90	111.71	90	569.21	25.20	0.013
2	Mono	13.7341	6.1305	6.9560	90	93.62	90	584.50	22.70	0.017
3	Mono	15.0443	6.1388	6.9588	90	113.89	90	587.61	18.50	0.004
4	Ortho	18.6097	12.9869	8.0763	90	90	90	1951.90	13.00	0.008

The best estimate of the unit cell was achieved by a monoclinic cell with a = 7.3755, b = 13.8282, c = 6.0073 Å and β = 111.71°. However, no distinctly independent "best" result was achieved and no outstanding M20 figure-of-merits were attained for any of the tested unit cells.

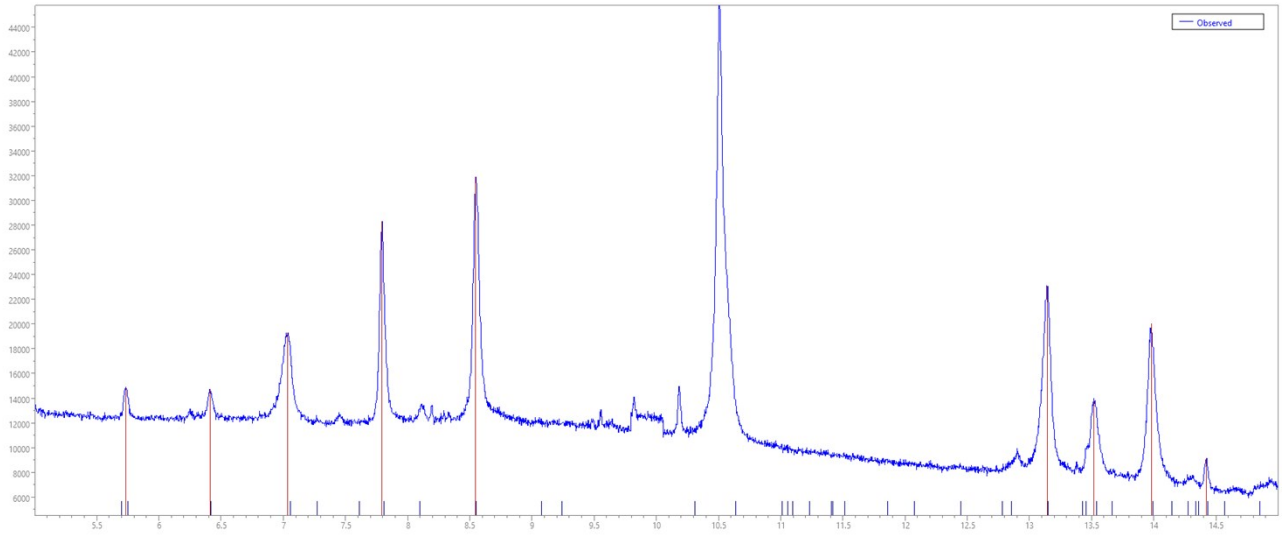

Figure S9. Selected region of the diffraction pattern of SWO 75% discharge at 600 °C. The red lines indicate the indexed peak positions of phase C and the blue ticks in the bottom indicate the Bragg positions of the best figure-of-merit monoclinic unit cell in the search.

References

[1] A. Altomare, C. Cuocci, C. Giacovazzo, A. Moliterni, R. Rizzi, N. Corriero and A. Falcicchio, *J. Appl. Crystallogr.*, 2013, **46**, 1231-1235.

[2] A. Boultif and D. Louer, *J. Appl. Crystallogr.*, 2004, **37**, 724-731.